Thesis: Numerical Simulations to Evaluate The Steering Capacities of Soft Robotic Probe in Dry Sand

Licheng Guo
Email: l.guo-1@student.utwente.nl

Supervisors:
Dr.ir Floriana Anselmucci
Email: f.a.r.anselmucci@utwente.nl

Dr.ir Ilya Brodoline
Email: i.b.brodoline@utwente.nl

Second Assessor:
Dr.ir Erik Horstman
Email: e.m.horstman@utwente.nl

Bachelor of Civil Engineering
University of Twente
July 2024

Abstract

This thesis investigates the steering capacities of a rigid tip designed for a soft robotic probe in dry sand, emulating the penetration mechanism inspired by earthworms. Using the Finite Element Method (FEM) within COMSOL Multiphysics, the study explores how variations in soil parameters and probe configurations affect effective stress distributions. The research focuses on two primary scenarios: penetration angles and bending maneuverability. Sensitivity analyses were conducted to assess the impact of soil density, Young's modulus, and bending displacement on effective stress. Findings indicate that while changes in Young's modulus and bending displacement significantly affect effective stress, while variations in soil density do not. This suggesting potential limitations in COMSOL's inbuilt calculation methods. The results provide insights for designing more efficient and durable rigid tips for soft robotic probes in soil exploration.

Contents

List of Figures

List of Tables

1. Introduction

The past decade has seen a surge in global challenges, including climate change, resource depletion, and energy transition. These challenges necessitate the development of novel, and sustainable solutions for soil characterisation, sensors and utility deployment and maintenance, as well as, tunnelling in areas inaccessible with traditional methods. To address these challenges, biotechnics, the interplay of biology, biological process, and geotechnical engineering, has become a new frontier (Liu et al., 2023).

In response to these challenges, nature offers a wealth of inspiration through biological adaptations. Worms and annelids rely on peristalsis to accomplish subterranean tunnelling for predator survival and offspring reproduction, such as earthworms, polychaetas, and inchworms (Zhang et al., 2024). For example, earthworms leverage their soft bodies and peristaltic movement to burrow and navigate through soil. By studying these natural processes, more perception can be gained for the design of geo-probes and soft robots.

Knowing that bioinspired soft robotics can significantly contribute to the geotechnical field, especially in regions like the Netherlands facing a constant risk of soil subsidence (Erkens & Stouthamer, 2020). Soft robotic probes could perform in-situ testing and characterisation of soil properties at previously inaccessible depths. This would enhance structural safety and stability while optimising resource allocation and construction costs in regions like the Netherlands, where robust foundations are important.

This thesis investigates the steering capabilities of a rigid probe, which originally represents the tip of an earthworm-inspired soft robotic probe, in dry sand. It begins with a chapter on research motivation and the problem statement related to soft robots and finite element methods. The literature review covers soft robotics, numerical methods, Mohr-Coulomb model, and cone penetrating tests. The research aims and questions are outlined, emphasising the primary and sub-research questions guiding the research. The research framework is outlines a comprehensive methodology that includes soil data collection through sieving analysis, void ratio analysis, and direct shear testing, along with the numerical simulation setup in a 3D environment and probe design analysis. Moreover, results include validation, soil domain size effects, and outcomes from penetration angle and steering scenarios. The discussion section interprets findings, and conclusions offer recommendations for further research. Furthermore, appendices provide detailed soil data, material properties of the probe, and COMSOL interface specifics along with geometry setup.

2. Context

2.1 Research Motivation

The current standard for subsurface investigation in civil engineering is the cone penetration test (CPT). This test serves multiple purposes, such as, identifying sub-surface layers and materials, as well as, estimating geotechnical parameters (Lunne et al., 1997). However, modern infrastructure projects often face complex challenges due to unpredictable subsurface conditions and potentially inaccessible environments.

This research explores the potential of bio-inspired soft robotics as a means to overcome the limitations of conventional CPT methods. Furthermore, the thesis specifically investigates the tip chamber component of the earthworm-inspired soft robotic probe, which a prototype of the soft robot is shown in Figure 2.1. Moreover, the investigation is done through numerical simulation, finite element method and the relevant literature review is presented in chapter 3.

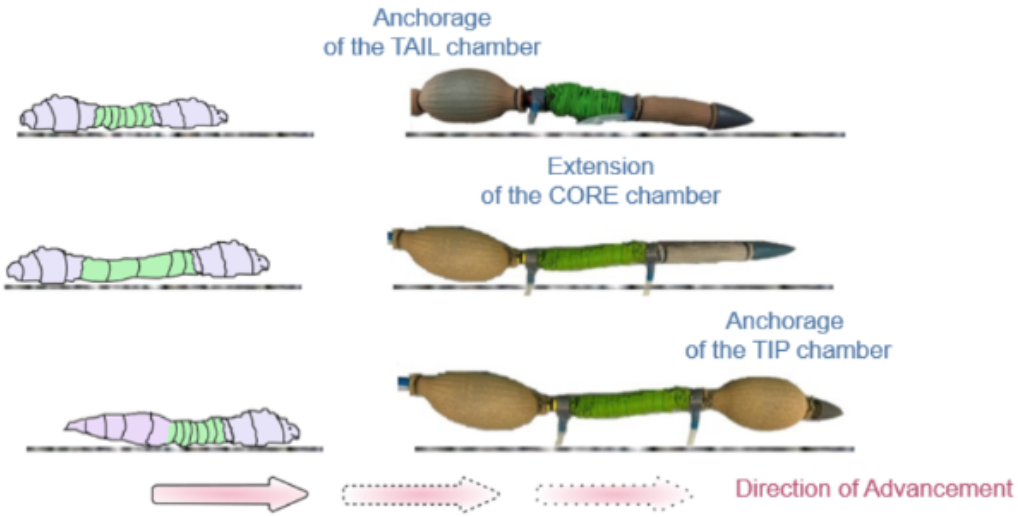

Figure 2.1: Left: Movement Pattern of an Earthworm. Right: Prototype of Earthworm Robot (Anselmucci et al., 2022).

2.2 Problem Statement

Optimizing the design of soft robotic probes is critical for enhancing their operational effectiveness. Research shows that soft robotic probes with optimized tip chamber designs can experience notably lower drag forces compared to traditional CPT probes (Patino-Ramirez & O'Sullivan, 2022). However, this thesis specifically targets the assessment of how soil affects the tip chamber of a soft robot, represented as a rigid probe, in its capacity to penetrate and rotate within it. Moreover, comprehending the resistance forces necessary for the rigid probe to manoeuvre and change its trajectory within the soil is important for improving its excavation efficiency.

3. Literature review

The scope of this thesis focuses on the rigid probe that imitates the tip of a earthworm soft robotic probe and its role in soil excavation. This innovative approach utilizes bio-inspired probes for soil exploration. Finite Element Method (FEM), a numerical method, is employed to analyze the behavior of these probes. The chosen numerical method incorporates relevant soil properties, including considerations for soil constitutive models like the one presented by Mohr-Coulomb (Coulomb, 1776). Ultimately, this research aims to position itself as an advancement over traditional methods like the cone penetration test (CPT) by offering a more efficient and less disruptive approach to soil characterization.

3.1 Soft Robot

Within the scope of soil exploration research, soft robotics emerges as a prospective field. Soft robots, constructed from pliable materials, present an innovative solution for navigating intricate environments while using less space than other locomotion types (Isaka et al., 2019). Specifically tailored for soil exploration, soft robotic probes offer several advantages. Firstly, their flexibility allows for seamless adaptation to the soil's contours, thereby mitigating the risk of disrupting its structure during penetration. Additionally, these robots excel in accessing confined spaces, navigating narrow crevices, or uneven terrain that conventional rigid probes may struggle to reach. Thus, within the context of soil exploration, soft robotics holds immense potential for revolutionizing exploration methodologies and advancing our understanding of subterranean environments (Isaka et al., 2019).

3.2 Numerical Method – Finite Element

In the context of this thesis investigating the effectiveness of rigid probes for soil exploration, the Finite Element Method (FEM) is chosen as the primary numerical analysis tool for several compelling reasons (Zienkiewicz et al., 2005). FEM offers versatility for handling complex geometries inherent in soft robotic probes, often inspired by biological designs. By discretizing these intricate geometries into smaller, simpler elements (finite elements), FEM enables accurate analysis of stresses, strains, and forces across the entire probe structure. Furthermore, FEM allows for the incorporation of various material properties into the model, which is crucial for simulating the behavior of the probe accurately. Moreover, FEM facilitates the modeling of the interaction between the probe and the surrounding soil. By defining appropriate material properties and boundary conditions for the soil domain, FEM enables the analysis and assessment of the forces experienced by the probe during penetration, thus evaluating its overall effectiveness. Additionally, FEM stands out for its accessibility and user-friendliness. Several FEM software packages like COMSOL can effectively simulate geotechnical excavation conditions (Han & Ma, 2019). They offer intuitive interfaces and extensive documentation. This makes them suitable for bachelor thesis research projects (Fong, 2019).

3.3 Mohr-Coulomb

In this research on investigating the tip chamber used for exploring the dry sand environment, the Mohr-Coulomb theory plays a crucial role. This theory helps understand how soil behaves under stress by linking the shear stress and the normal stress on a soil element, which helps predict when it might fail as shown in Figure 3.1.

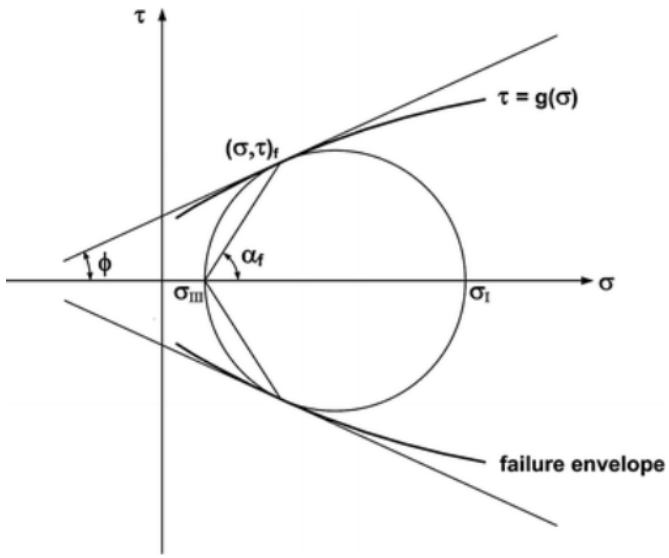

Figure 3.1: Mohr-Coulomb Failure Criterion (Labuz & Zang, 2012).

Furthermore, each symbol is represented as the followings:

- τ (Shear Stress): This is the stress component that acts parallel to the plane of interest within the soil. It measures the force that causes layers of the soil to slide past one another.
- σ (Normal Stress): This is the stress component acting perpendicular to the plane of interest. It measures the force exerted per unit area within the soil, either compressive or tensile.
- α_f (Cohesion Intercept): This parameter represents the inherent shear strength of the soil material even in the absence of any normal stress ($\sigma = 0$).
- ϕ (Friction Angle): This is the angle of internal friction of the soil. It represents the slope of the failure envelope and is a measure of the soil's resistance to shearing along internal planes.
- c (Cohesion): This is the intercept of the failure envelope on the shear stress axis when the normal stress is zero. It represents the cohesive strength of the soil.

The *failure envelope* in the $\sigma - \tau$ plane is a crucial concept within the Mohr-Coulomb theory. It is a boundary line that separates a safe zone from a failure zone. The failure envelope is typically represented by a straight line defined by the following equation:

$$\tau = \sigma \times \tan(\phi) + c \tag{3.1}$$

The Mohr-Coulomb theory gives a way to understand how dry sand reacts to the stresses caused by the probe's movement. When utilizing techniques like Finite Element Analysis (FEM) to simulate the behavior of probes in dry sand, the Mohr-Coulomb theory serves as a crucial tool for interpreting the outcomes. By examining how stress is distributed throughout the simulated soil, the performance of varying penetration directions and rotation maneuverability on the probe's can assessed.

3.3.1 Cone Penetrating Test

Cone penetration testing (CPT) is a widely used technique in geotechnical engineering for understanding soil properties (Lunne et al., 1997). If these probes achieve similar penetration depths and provide data that correlates well with CPT results, it strengthens their potential as a valuable alternative. It's important to note that CPT offers valuable information, but it can be disruptive. The rigid cone penetrometer can cause significant disturbance to the soil structure, which potentially affecting the accuracy of collected data. Soft robotic probes, with their flexibility, offer the potential to minimize soil disruption while still providing useful data about the soil environment.

4. Research Dimensions

4.1 Research Aim

This study aims to investigate how dry sand soil affects the steering capabilities of a rigid probe tip. The results can inform the design of soft robotic probes to achieve efficient soil penetration.

4.2 Research Question

The primary objective of this research is to investigate how dry sand affects the steering capabilities of a rigid probe tip for efficient soil penetration. This study utilizes finite element modeling (FEM) conducted with COMSOL software. The following sub-research questions will guide the investigation.

4.2.1 Main Research Question

> "How does dry sand soil influence the steering capabilities of a rigid probe tip for efficient soil penetration, as assessed through finite element modeling (FEM) using COMSOL software?"

4.2.2 Sub-Research Questions

- Are there available experimental results related to rigid probe tips in dry sand that can be used to validate the accuracy of the COMSOL simulations?
- How can appropriate boundary conditions be defined in COMSOL to represent the interaction between the probe tip, the dry sand domain, and the surrounding environment?
- How do different changes in penetration direction affect the magnitude and distribution of resistance forces?
- How can we simulate the steering capability of the probe tip using FEM?
- What are the resistance forces experienced by the probe tip during steering and penetration in dry sand?

5. Research framework

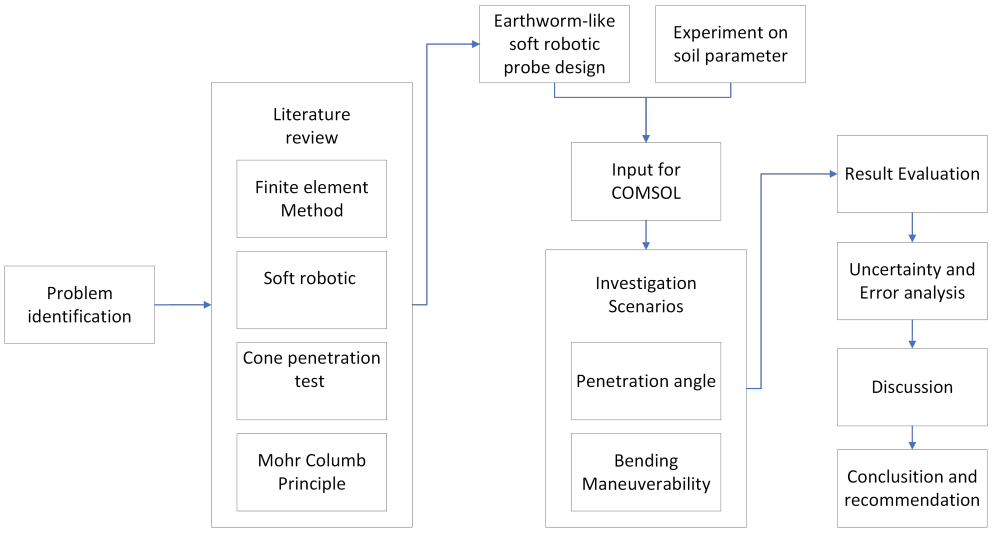

Figure 5.1: Research Framework for Evaluating Steering Capacities of a Soft Robotic Probe

The research framework, shown in Figure 5.1, builds upon existing knowledge across critical areas to address the identified problem. Initially, a comprehensive literature review is conducted, focusing on four main topics: the finite element method (FEM), soft robotics, the cone penetration test (CPT), and the Mohr-Coulomb principle. This review helps identify successful strategies and limitations, informing the development of a bioinspired soft robotic probe.

The literature review helps understand the design of an earthworm-like soft robotic probe and the necessary experiments on soil parameters. These experiments provides essential input for the COMSOL Multiphysics simulations. The FEM within COMSOL analyzes the probe's behavior in dry sand under various conditions, which are change in penetration angles and bending maneuverability.

The investigation scenarios focuses on two main aspects: penetration angle and bending maneuverability. Firstly, penetration angle is examined to assess how different angles impact the effective stress experienced by the rigid probe. Secondly, bending maneuverability is evaluated to understand the probe's steering capabilities and stress distribution during different bending maneuvers. This analysis provides perceptions into optimizing the probe's design for effective soil exploration.

The evaluation leads to a detailed discussion of the results, highlighting the practical implications for designing soft robotic probes. The conclusion and recommendations for future works provide insights into the steering capacity of the rigid tip, which represents the tip chamber of the earthworm soft robot.

6. Methodology

This chapter outlines the methodology used to investigate the steering capacities of a rigid probe tip for a soft robotic probe in dry sand, covering soil data collection, experimental setup, numerical simulation setup, and probe design analysis. The soil data collection includes sieving analysis, void ratio analysis, and direct shear testing to characterize soil properties. This ensures accurate boundary conditions and material properties for the numerical simulations. The experimental setup is used to validate the result of the FEM simulation. The 3D numerical simulation setup, provides a more accurate representation of the experimental setup compared to 2D models. The probe design section explains the geometric modeling in COMSOL. To avoid anomalies, a smooth outline of the geometry is used, as explained in Appendix C, and the probe is divided into small disks to simulate bending and steering maneuvers. Various steering scenarios are presented to evaluate the probe tip's performance under different conditions.

6.1 Soil Data Collection

6.1.1 Soil Particle Distribution

Sieving analysis is important for particle size distribution analysis, as well as for understanding granular materials (American Society for Testing and Materials (ASTM), 2007). In this research, sieving analysis helps in simulating the rigid probe designed to investigate its steering capacities within dry sand. This research adheres to established methodologies used widely for sieving analysis in soil, ensuring consistency and comparability with similar work (American Society for Testing and Materials (ASTM), 2007).

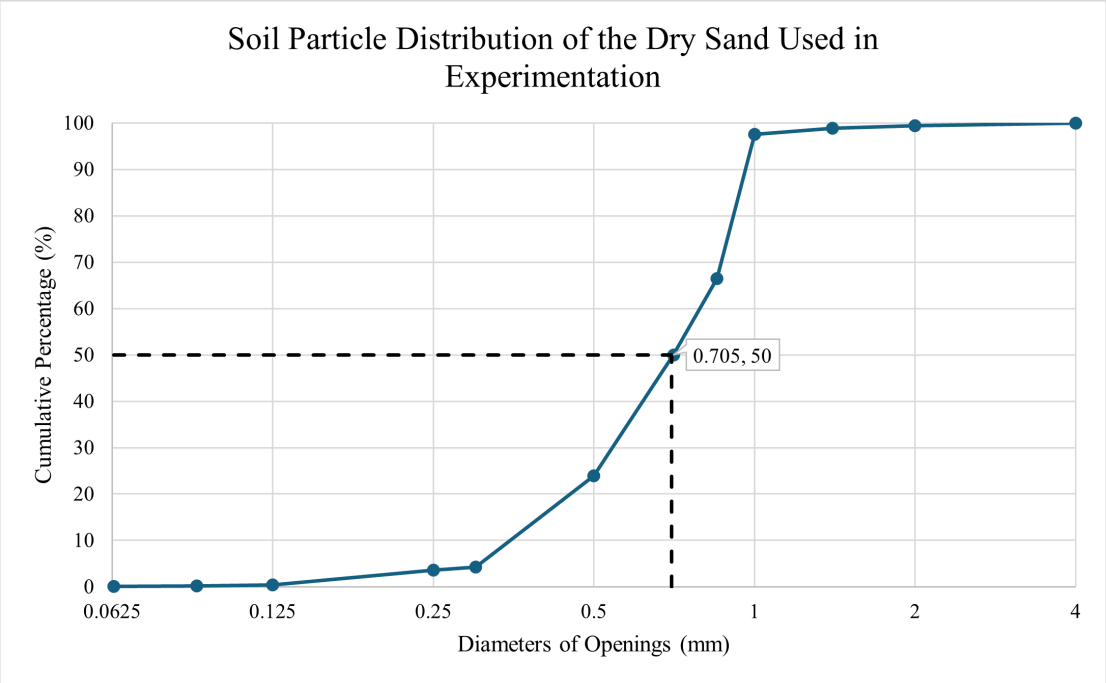

Figure 6.1: Soil Particle Distribution of the Dry Sand Used for Experiments

The sieving analysis is performed utilizing a standard sieving machine. The procedure entailed the preparation of soil samples, which are then loaded into the sieving apparatus and processed through a series of progressively finer sieves. The mass of particles retained on each sieve is meticulously recorded to determine the particle size distribution. As shown in Figure 6.1, the sieving analysis results indicate that the median particle diameter (D_{50}) of the soil sample is 0.705 mm.

6.1.2 Void Ratio Analysis

Soil void ratio analysis is an important aspect of soil mechanics. It provides insights into the density and compaction characteristics of granular materials. This analysis is crucial for simulating the behavior of the rigid probe within dry sand, as it helps establish the necessary boundary conditions for accurate modeling. The void ratio, defined as the ratio of the volume of voids to the volume of solids in a soil sample, is determined using standardized methods to ensure consistency and reliability.

The soil void ratio analysis is conducted in accordance with ASTM standards D4253-16 and D4254-06. These standards specify the procedures for determining the maximum (e_{max}) and minimum (e_{min}) void ratios of granular soils. The procedure involved the following equation and steps:

$$e = \frac{V_{\text{total}} - V_{\text{solid}}}{V_{\text{solid}}} \tag{6.1}$$

where V_{total} is the total volume of the container and V_{solid} is the volume of the soil solids.

1. **Sample Preparation:** Soil samples are carefully prepared to ensure homogeneity and representativeness.
2. **Maximum Void Ratio (e_{max}):** The soil sample is loosely placed in a container, and its volume is measured. The void ratio is calculated based on the known volume of the container and the mass of the soil using the equation:
3. **Minimum Void Ratio (e_{min}):** The soil sample is compacted to its densest state using a shaker table. After compaction, its volume is measured, and the void ratio is calculated using the same equation.
4. **Repetition and Data Recording:** The experiment is repeated three times to ensure accuracy and reliability. The detailed data from these repetitions can be found in Appendix A.

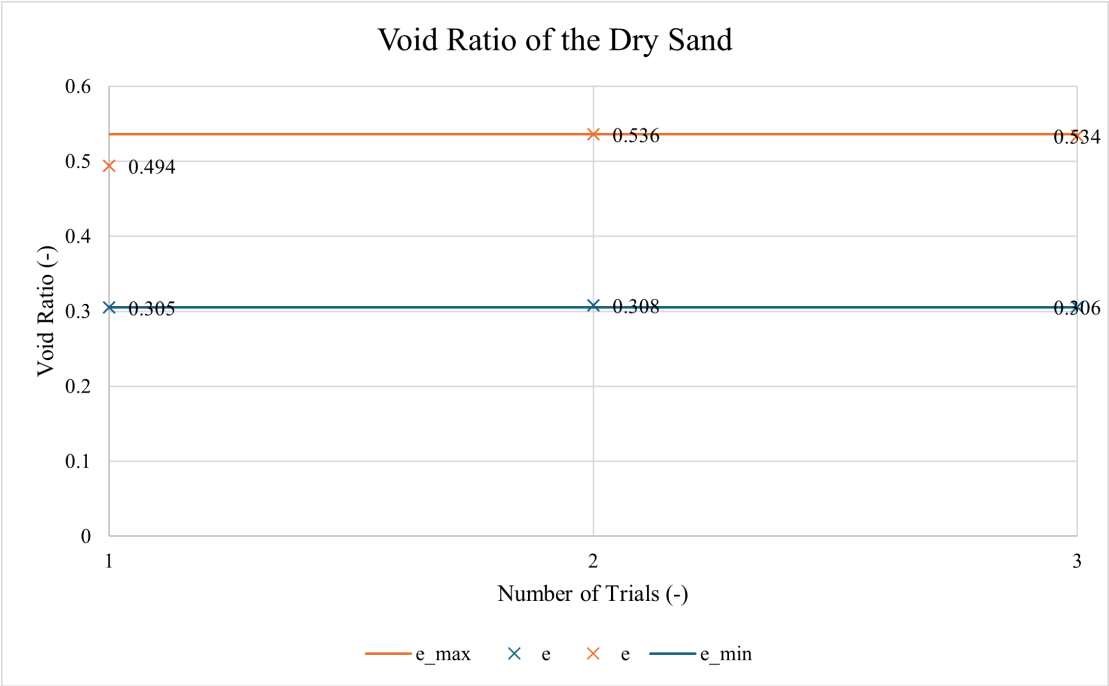

Figure 6.2: Void Ratio of the Dry Sand

The results of the soil void ratio analysis indicate that the maximum void ratio is 0.536 and the minimum void ratio is 0.305 as shown in Figure 6.2. These values are selected from the three repeated experiments to ensure precision. These findings are critical for simulating the elastoplastic interactive behavior of soil and the probe.

6.1.3 Direct Shearing Test

The shear stress of the soil is determined using ELE International soil testing equipment. The apparatus is connected to a data logger, which requires the following inputs to perform the shear test: shear box area, sample height, sample weight, weight applied, and stress applied. The shear test is then performed with different normal stress, and the maximum shear stress is identified.The weights applied on the equipment are 20 N, 40 N, and 80 N, which correspond to normal stresses of 22.1 kPa, 28.5 kPa, and 41.2 kPa, respectively, including the weight of the equipment hanger. A sample calculation can be seen in Appendix A.2.

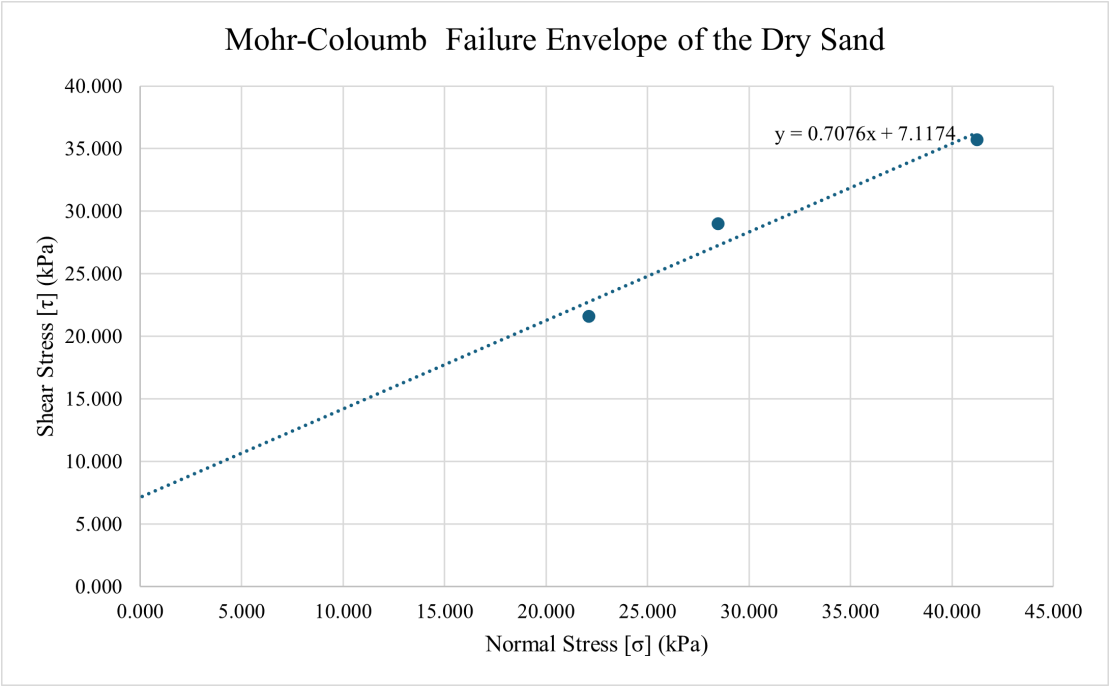

Figure 6.3: Mohr-Coloumb Failure Envelope, Indicating the Cohesion and the Friction Angle of the Dry sand Used for the Experiments

As shown in Figure 6.3, a linear interpolation is plotted along with its corresponding linearized equation relating maximum shear stress (τ) and normal stress (σ). This equation allows for the determination of cohesion (c) and friction angle (ϕ). In this case, the analysis yielded a cohesion value of 7.12 and a friction angle of 35.3°, which is determined through the trend line. This is correlated with Equation 3.1.

6.1.4 Summary of Soil Parameter Values

Table 6.1 shows the overall results of the soil properties, which is used in the next section to set up the COMSOL simulation. This detailed characterization includes important parameters such as the median grain size (D_{50}), maximum and minimum void ratios, cohesion, and friction angle.

Table 6.1: Soil Properties

Property	**Value**	**Unit**
D_{50}	0.705	mm
Void ratio [max]	0.536	-
Void ratio [min]	0.305	-
Cohesion	7.12	kPa
Friction angle	35.3	degrees

These properties provide a clear understanding of the soil's physical and mechanical behavior, which is essential for accurately modeling the interaction between the soil and the probe. By integrating these values into COMSOL, the probe's performance can be simulated under realistic

conditions. This data-driven approach allows for precise calibration of the simulation model, as well as helping in the investigation of the probe's steering capabilities and overall effectiveness in soil penetration tasks.

6.2 Experiment Setup

To validate the FEM simulation, an experimental setup is created to ensure comparable results.

Figure 6.4: The Experiment setup (Tekin, 2024)

The experimental setup, shown in Figure 6.4, uses dry sand and includes tests for direct shear, void ratio, and soil particle size. The soil domain is cylindrical, with a radius of 12 cm and a depth of 78 cm. Additionally, the rigid probe displaces 20 cm, driven by a motor. A sensor located at the tip of the probe measures the experienced stress. For further details on the experimental setup and its effects, refer to Tekin (2024).

6.3 Numerical Simulation Setup

This section outlines the numerical simulation setup in COMSOL. The model is built in a 3D environment instead of a 2D plane or 2D asymmetry. Using 3D modeling provides a more accurate representation of the experiment. In a 2D plane model, the system assumes an infinitely extended version of the geometry, which misrepresents a cylindrical soil domain as a rectangle. Additionally, 2D asymmetry is unsuitable for this study, which involves changes in penetration angle as shown in sub-section 6.3.2. In 2D asymmetry, there is only one line of revolution that can be used. A line of revolution is an axis around which the geometry is rotated to create the 3D shape. Since it requires two lines of revolution to accurately represent the changes in the probe's penetration angle, with one line of revolution being used for creating the soil domain, the model

prevents accurate modeling of these changes. Therefore, a 3D model is used to provide a more precise representation of the probe's behavior under varying penetration angles. The trade-off for the improved accuracy of 3D modeling is significantly higher computation time compared to 2D modeling. Additionally, the risk of obtaining non-converging results is significantly higher, which can hinder the development of the simulation.

6.3.1 Soil Domain

The soil domain in this numerical simulation is treated as elastic. The model represents the soil domain as a cylinder with a diameter of 12 cm and a depth of 78 cm. This setup accurately reflects the experimental conditions, where the soil is penetrated to a depth of 20 cm. The simulation is displacement-driven, which means the soil displacement is controlled to mimic the experimental penetration.

The boundary conditions play an important role in ensuring the accuracy and reliability of the simulation. The sides of the cylindrical soil domain are treated as roller, while the bottom is also fixed to simulate the natural confinement of soil. This setup ensures that the simulation accurately represents the physical constraints experienced by the soil during the experiment.

COMSOL presents the von Mises stress after the numerical simulation, which is depicted in Figure 6.5. Von Mises stress is an important parameter because it represents the effective stress in the material. In the context of this simulation, the von Mises stress shows the distribution and magnitude of stress within the soil, which is essential for understanding the interaction between the probe and the soil.

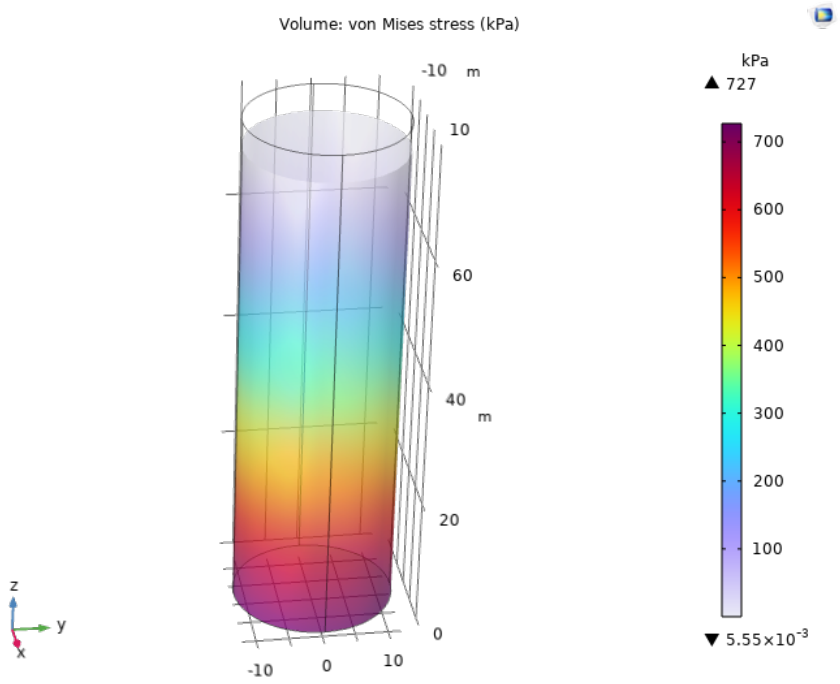

Figure 6.5: Display of Yield Stress of Soil Domain in COMSOL

The von Mises stress is particularly useful because it combines the three principal stresses into a single equivalent stress value, making it easier to analyze the material's response under complex loading conditions. This stress measure is crucial for comparing the simulation results with

experimental data.

The soil in the simulation is characterized by several key material properties:

- Poisson's ratio: This parameter reflects the soil's elasticity and its tendency to expand or contract perpendicularly to the direction of compression or tension.
- Young's modulus: This measures the soil's stiffness and resistance to deformation.
- Density: This property affects the overall mass and inertia of the soil.

The simulation is stationary, meaning it assumes a steady-state condition where the soil properties and stresses are constant over time. This approach is chosen to simplify the analysis and focus on the static interaction between the probe and the soil, rather than dynamic changes over time.

The results of the numerical simulation is compared and validated against experimental results. In the experiment, the soil domain is a cylinder with a diameter of 12 cm and a depth of 78 cm. The probe penetrates the soil to a depth of 20 cm, and the simulation is displacement-driven to replicate this process. The stress at the probe tip in the simulation is compared to the maximum stress reached at 20 cm of displacement in the experiment. This comparison validates the accuracy of the simulation while reliably ensuring the physical behavior of the soil-probe interaction.

6.3.1.1 Investigate the Size of the Soil Domain

In further development of the numerical simulation objectives of this study, it is imperative to analyze the influence of the soil domain boundary. The stress distribution in the soil is significantly affected by the boundary conditions, particularly the diameter of the soil domain. Therefore, simulations focusing on varying the radius of the soil domain from 10 cm to 50 cm are conducted. The primary goal is to mitigate the influence of the soil domain boundary on the investigation of the probe tip's steering capacity. This allows for a more focused investigation of the probe's behavior within the soil domain.

6.3.1.2 Soil Model Limitation

The decision not to treat soil behavior as elastoplastic roots from the challenge of achieving convergent results within the simulation framework. This limitation necessitates the adoption of alternative modeling approaches to ensure the stability and accuracy of the numerical analysis. The parameter values utilized in the simulation are documented in Appendix C. Additionally, the simulation is executed in a stationary mode to address specific computational constraints and ensure the feasibility of the analysis. This choice is made in consideration of the computational resources available and the complexity of the simulation setup.

6.3.2 Probe Design

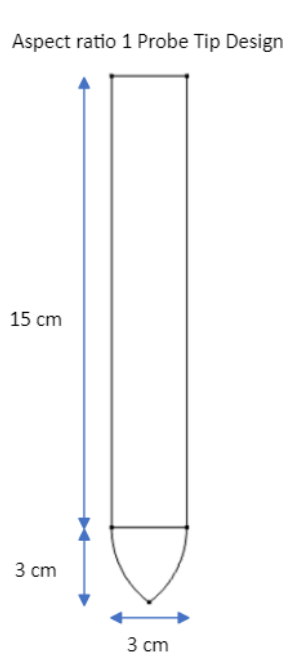

(a) Probe Design with Aspect Ratio 1

(b) The Cone Penetrometer (Geoprobe, n.d.)

Figure 6.6: Probe Design Used in the COMSOL Simulation Compared to a Cone Penetrometer (Geoprobe, n.d.)

The probe used for the simulation is shown in Figure 6.6a. It should be noted that this probe is designed to emulate a cone penetrometer, which is shown in Figure 6.6b. The probe has a rigid body made from PLA, amd its material properties are shown in Appendix B. The probe's length is 18 cm, and its diameter is 3 cm. The tip design has an aspect ratio of 1, meaning the height of the tip is equal to the diameter of the probe, which serves as the reference design. Furthermore, the measurement points of the effective stress are located at each joint of the disks.

In COMSOL, the geometry of the probe tip is modeled using a revolution technique. This involves creating a smooth outline of the probe tip and then revolving it around the z-axis to generate the three-dimensional geometry. The decision to create a smooth outline helps to avoid minuscule empty spaces between adjacent geometries. These spaces can lead to exaggerated results during numerical simulations, particularly when the mesh size is too large. In such cases, the particles may attempt to fit into these empty spaces, resulting in anomalies in the displayed results. For clarity, the detailed implementation of the geometry interface is provided in Appendix C. This interface offers insights into the precise modeling techniques employed to ensure the reliability of the simulation outcomes.

6.3.2.1 Steering Capacity Investigation Scenario 1: Penetration Angle

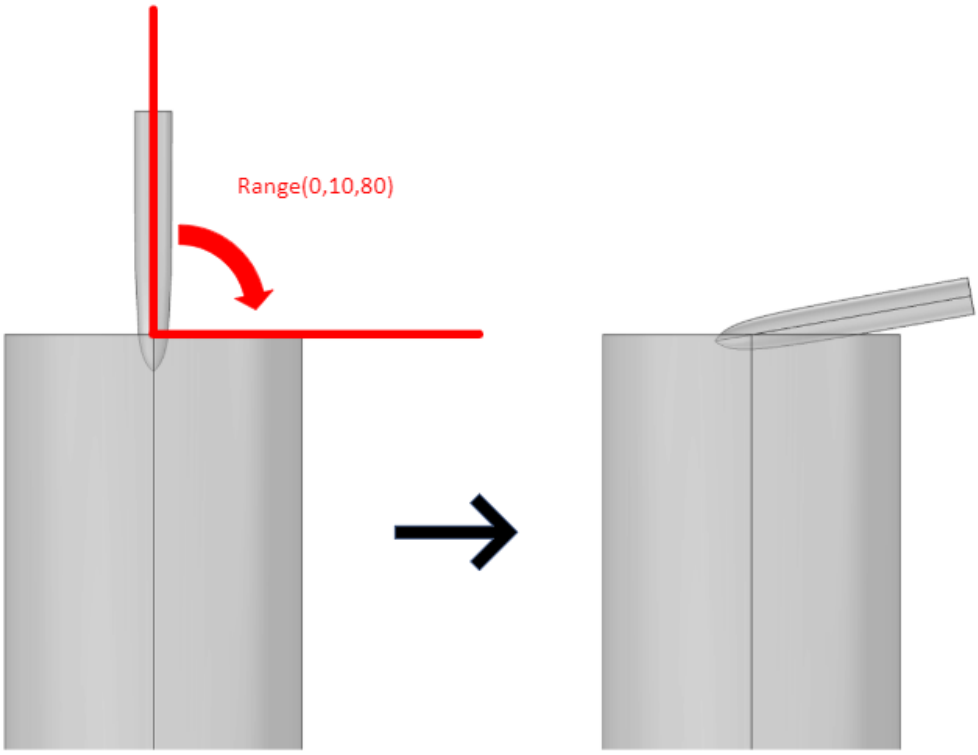

Figure 6.7: Illustration of Change in Probe's Penetration Angle

One scenario for evaluating the steering capacities involves examining the variation in stress as the penetration angle changes. As shown in Figure 6.7, this variation is initiated at the onset of displacement. The evaluation spans angles from 0 to 80 degrees, with increments of 10, relative to the normal angle between the soil domain surface and the probe. The limitation of not reaching a 90-degree angle is due to the probe being partially submerged in the sand, and it is moving only across the surface of the soil domain. Further investigation into the effects of horizontal penetration, both within and outside the soil domain, could provide additional insights.

6.3.2.2 Steering Capacity Investigation Scenario 2: Steering

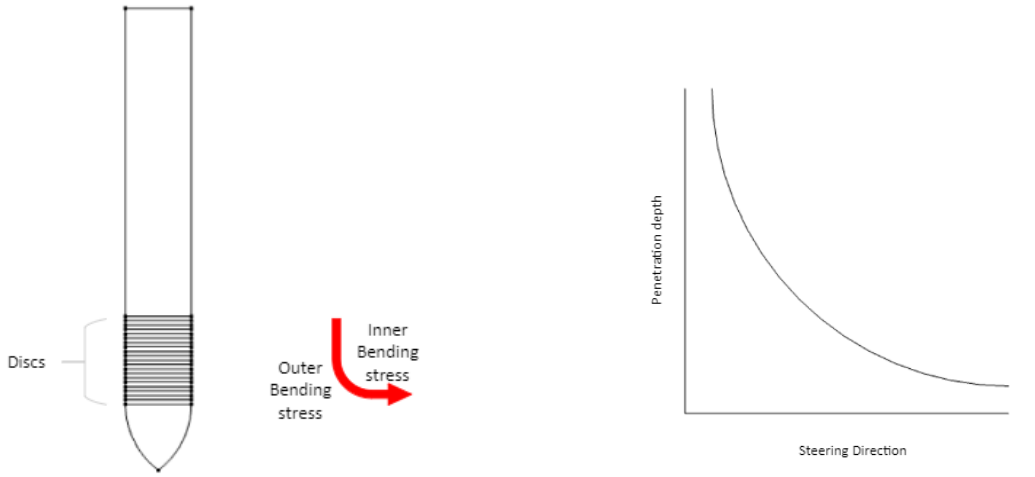

(a) Illustration of Probe with Multiple Disks

(b) Bending Radius of the Probe Tip

Figure 6.8: Illustration of Bending Rate

Another scenario involves investigating the stress imposed on the probe by the soil during a steering maneuver within the soil. To simulate this, the rigid body of the probe is divided into multiple small disks, as shown in Figure 6.8a. In COMSOL, steering is simulated by imposing bending displacement. The bending displacement is by applying different rates of displacement on each disk to imitate the bending motion. The rate of displacement is illustrated in Figure 6.8b, where the overall bending displacement forms a quarter of a circle, ensuring a 90-degree steering maneuver within the soil. Increasing the number of disks allows for more refined steering simulation, resulting in more accurate outcomes.

Technically, when a body bends, the outer side experiences tension while the inner side undergoes compression, altering the shape from a rectangle to a triangle from the side view of the disk. The labeling of the stress in highlighted in Figure 6.8a. However, this numerical simulation does not account for this deformation, and further studies could explore this aspect. This scenario is crucial for understanding the probe's steering capabilities and optimizing its design for effective soil navigation, which is further pointed out in the discussion chapter (8).

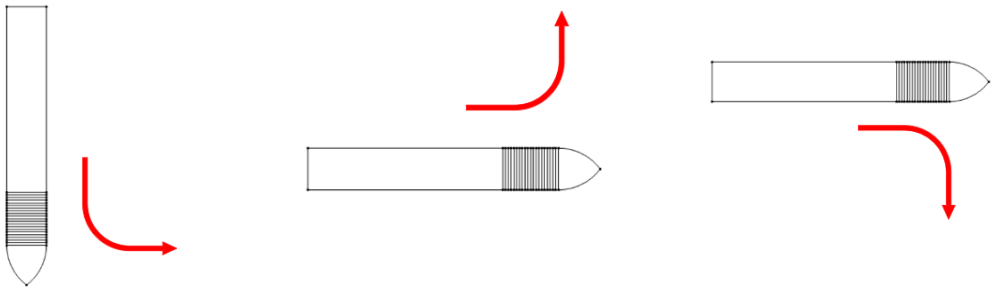

(a) Case 1: Bending - Vertical to Horizontal

(b) Case 2: Bending - Horizontal to Vertical - Upward

(c) Case 3: Bending - Horizontal to Vertical - Downward

Figure 6.9: Different Cases of Bending for the Investigation

Furthermore, there are three situations of steering maneuvers investigated, as shown in Figure 6.9. Case 1 (Figure 6.9a) describes bending the probe from a vertical orientation to a horizontal one. This maneuver is critical for understanding the stress distribution and the probe's ability to transition from a vertical penetration to a horizontal movement within the soil. Case 2 (Figure 6.9b) describes bending from a horizontal to a vertical position in an upward direction. This scenario helps evaluate the probe's capability to navigate upwards within the soil, which is essential for tasks such as reaching different soil layers or escaping potential obstacles. Case 3 (Figure 6.9b) describes bending from a horizontal to a vertical position in a downward direction, crucial for understanding how the probe can penetrate deeper into the soil or maneuver around obstacles below it. These varied bending scenarios provide comprehensive insights into the probe's steering capabilities by discovering the location of where the peak stress is experienced.

7. Results

7.1 Validation of Results

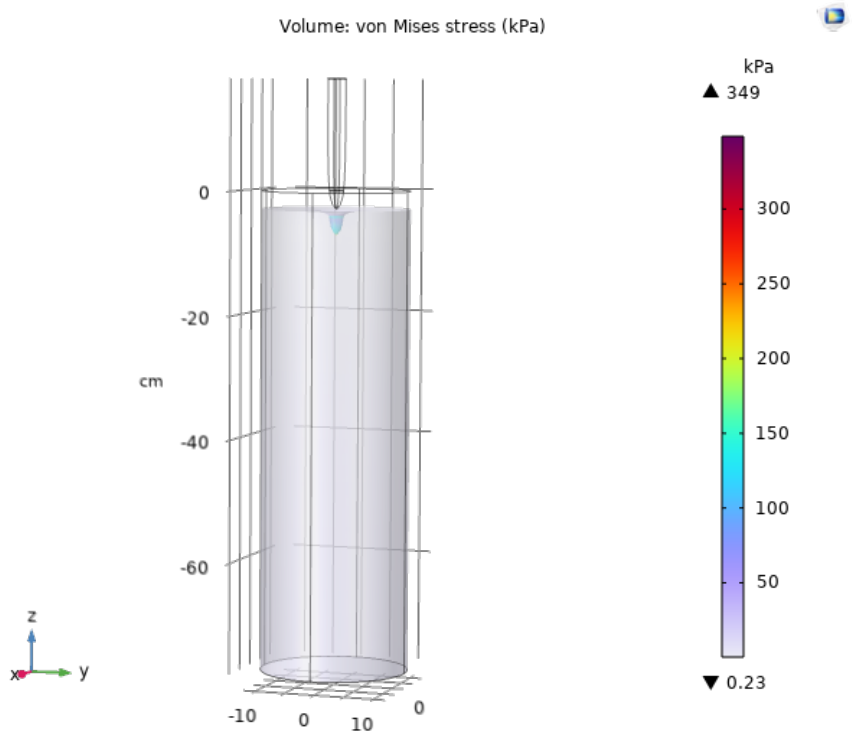

Figure 7.1: Numerical Simulation Result - The diagram shows the soil domain being penetrated by the rigid probe to a depth of 20 cm. The color map indicates the von Mises stress distribution in kPa, with stress values ranging from 0.23 kPa to 349 kPa.

To validate the simulation, the experimental value of 382 kPa for a probe with an aspect ratio of 1 is used for comparison. The simulation result, shown in Figure 7.1, indicates an effective stress of 349 kPa.

The close alignment between the simulation result and the experimental value suggests that the numerical model is reliable. More importantly, the material properties are adjusted, with the Young's modulus loaded by three orders of magnitude to achieve a similar stress magnitude at the probe tip. This adjustment is necessary to match the stress levels observed experimentally. The input parameter values are shown in Appendix C.

This validation confirms that, despite the modification in material properties, the simulation setup including boundary conditions and geometric representation accurately reflects the experimental conditions shown in Section 6.2. Therefore, the model can be used to explore the intended scenarios and analyze the probe's steering capacity performances.

7.2 Size of Soil Domain

The investigation of the size of the soil domain is conducted with a series of simulations to assess the influence of the soil boundary on stress distribution around the probe. The study varied the radius of the soil domain from 12 cm to 50 cm to observe how these changes impact the stress distribution experienced by the probe tip. The primary goal is to mitigate boundary effects that could affect the investigation of the probe tip's steering capacity, and the boundary that is determined optimal is used in further simulations.

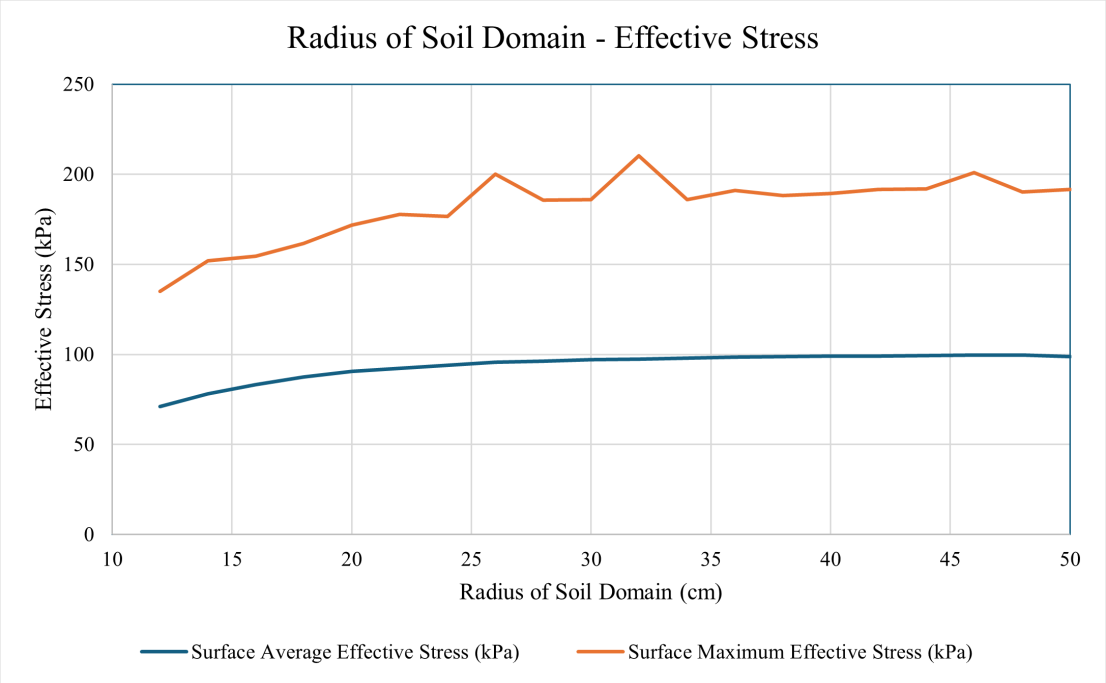

Figure 7.2: Radius of Soil Domain vs. Effective Stress in COMSOL Simulation - The graph indicates the relationship between the radius of the soil domain and the effective stress experienced by the probe, evaluating the influence of the soil domain boundary.

The result of the size of soil domain simulation, as shown in Figure 7.3, reveals critical insights into the stress distribution around the probe. The orange line in the graph represents the surface maximum effective stress values obtained from COMSOL simulations, where the tip of the rigid probe is buried in the soil before any displacement. The blue line indicates the surface average effective stress over the area.

The result indicates that a soil domain radius of 30 cm is optimal for the simulations. At this radius, both the surface maximum and average effective stress values begin to stabilize, suggesting that the boundary effects are sufficiently reduced. After 30 cm, further increases in the domain radius have minimal impact on the stress distribution, which indicates a point of diminishing returns.

The surface maximum effective stress (orange line) shows more ups and downs compared to the surface average effective stress (blue line) due to several reasons. COMSOL's finite element method is very sensitive to the mesh quality and density. A finer mesh gives more accurate results but needs more computational power, and on the other hand, a coarser mesh can cause noticeable fluctuations. Lastly, as the size of the soil domain changes, the boundary conditions

can affect how stress is distributed, especially at the edges where the probe touches the soil. These factors together cause the variations seen in the surface maximum effective stress.

7.3 Result of Scenario 1: Penetration Angle

Investigating penetration angles is essential to understand how different angles impact the stress distribution around the probe tip. This scenario examines the relationship between penetration angle and the effective stress experienced by the probe. By varying the penetration angles from 0 to 80 degrees, the results aim to analyze the relationship between in the penetration angle and the stress experienced by the probe.

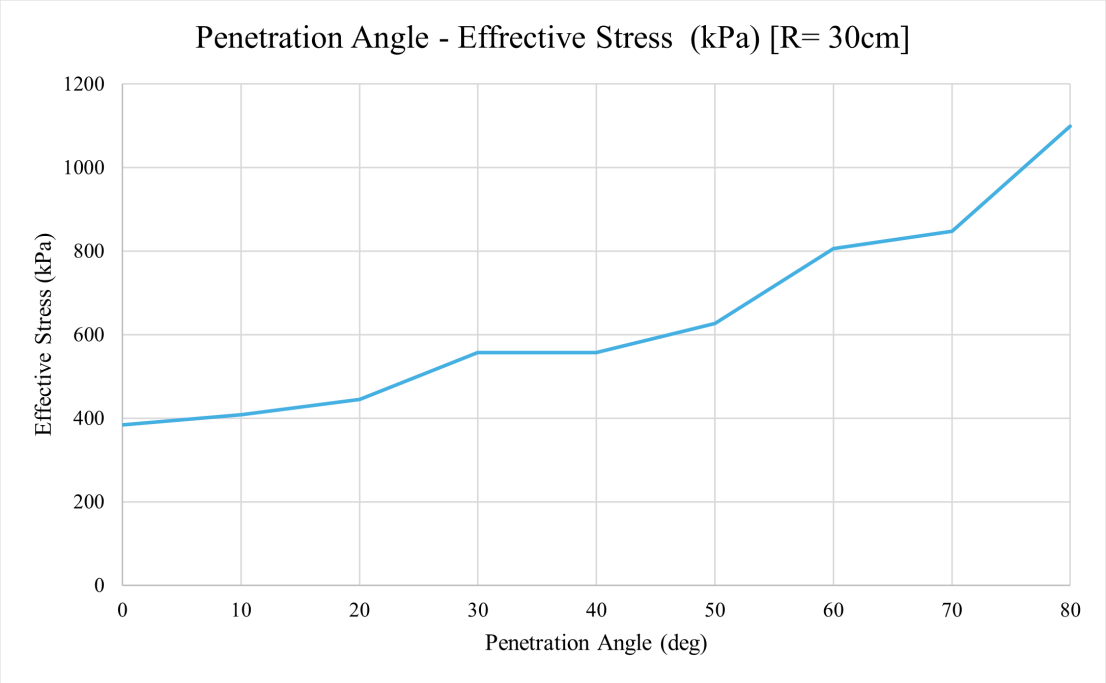

Figure 7.3: Relationship between Penetration Angle and Effective Stress for a Soil Domain with Radius 30 cm

The graph in Figure 7.3 illustrates the relationship between penetration angle and effective stress for a soil domain with a radius of 30 cm. As the penetration angle increases , there is a significant rise in effective stress. Initially, the effective stress remains relatively stable, showing only a slight increase up to 20 degrees. After this point, the stress begins to rise more significantly, reaching the peak at 80 degrees. This trend suggests that as the probe's penetration angle increases, the resistance from the soil increases due to the larger contact area and greater deformation of the soil. The gradual increase in stress up to 20 degrees indicates that small changes in penetration angle do not significantly impact the stress experienced by the probe, where steeper angles result in higher stresses, which can potentially affect the probe's durability.

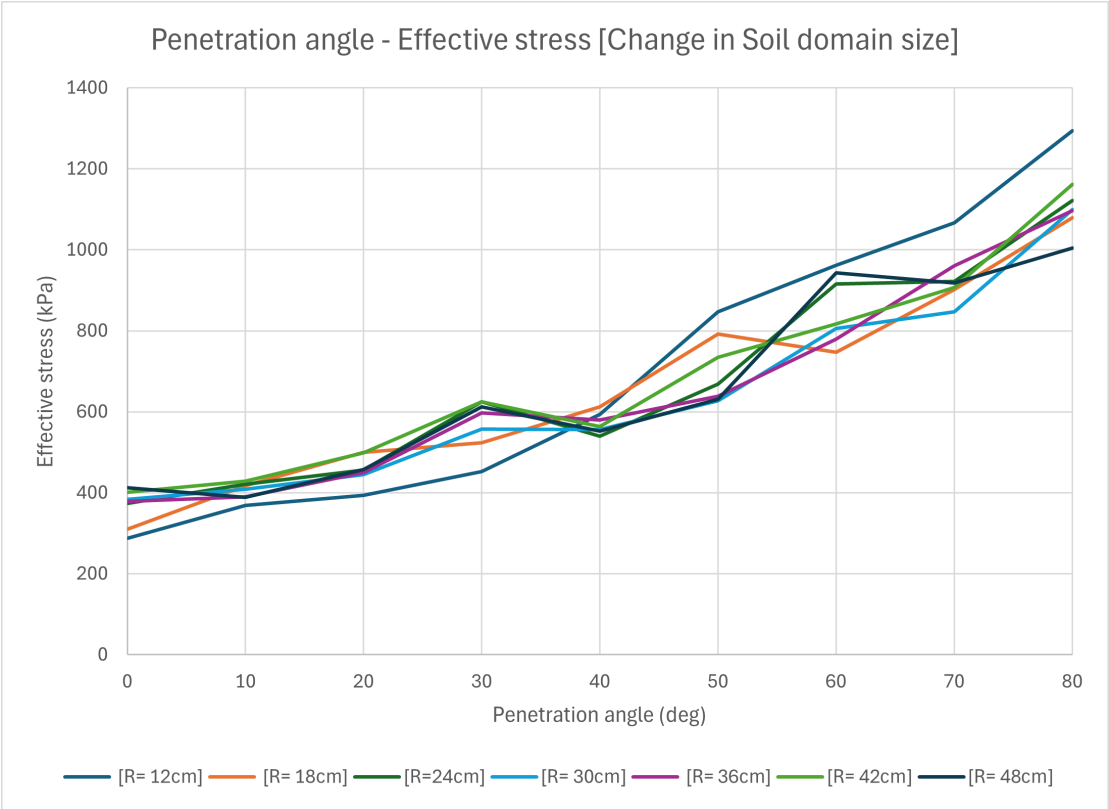

Figure 7.4: Relationship between Penetration Angle and Effective Stress Across Various Soil Domain Sizes

The graph in Figure 7.4 provides a more detailed analysis by showing the effective stress at different penetration angles across various soil domain sizes. The radius of the soil domains range from 12 cm to 48 cm. Similar to the Figure 7.3, there is a general trend of increasing effective stress with increasing penetration angles. However, the rate of increase and the absolute values of stress vary depending on the soil domain size.

For smaller soil domains (e.g., R=12 cm and R=18 cm), the effective stress increases more rapidly and reaches higher values at larger penetration angles. This could indicate that smaller soil domains may constrain the soil more tightly, leading to higher resistance and thus higher stress. Conversely, with larger soil domains (e.g., R=42 cm and R=48 cm), they show a more gradual increase in stress. This suggests that these larger volumes can better accommodate the probe's movement without experiencing excessive stress.

7.3.1 Implication of the Result for Probe's Steering Capacity

The result of penetration angle benefits the field of earthworm-inspired soft robots, which mimic the burrowing mechanisms of earthworms. By optimizing penetration angles and understanding stress distribution, these robots can excavates more efficiently, which reduces energy consumption and improving navigation through various soil types. The findings on material properties and stress management enhance the durability and operational life of these robots, making them more reliable for long-term applications.

7.4 Result of Scenario 2: Steering

It is important to understand the probe's steering maneuverability under different conditions to optimize the design for effective soil penetration and navigation. This section shows the results of the steering cases, examining the stress distribution along the probe during various bending maneuvers. This information is crucial for improving the probe's structural integrity and functionality, which ensures that the probe can withstand the forces encountered during practical applications. The following results highlight the stress behaviors observed in three distinct bending scenarios: bending from vertical to horizontal, bending from horizontal to vertical in an upward direction, and bending from horizontal to vertical in a downward direction.

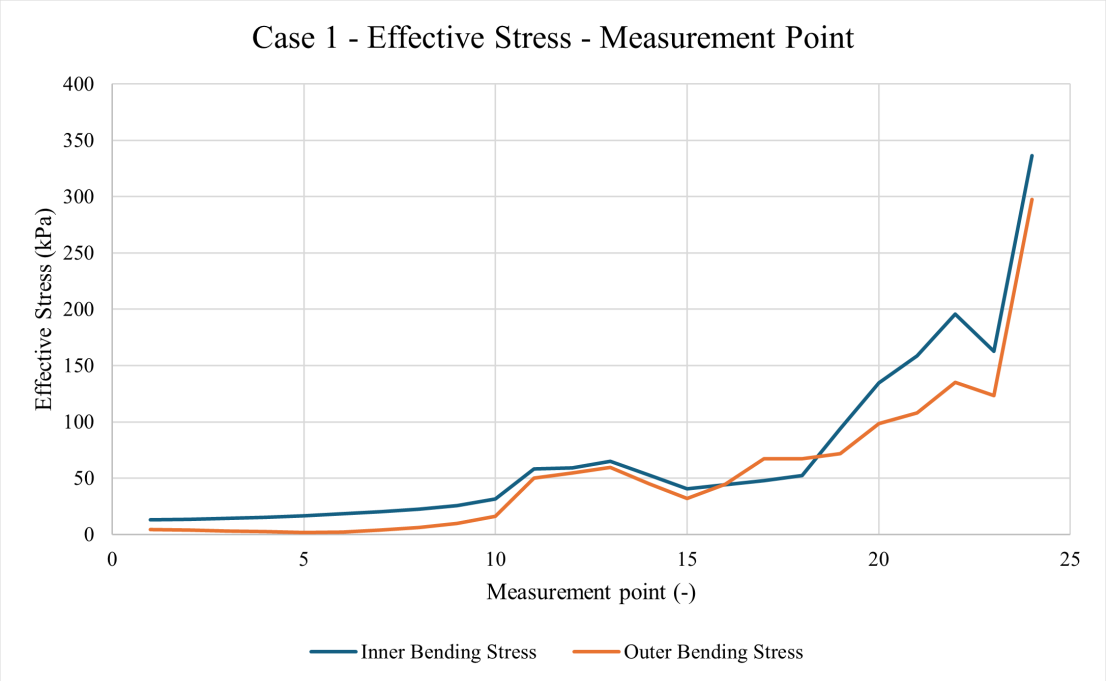

Figure 7.5: Result of Case 1 - Bending from Vertical to Horizontal

In case 1, where the probe bends from a vertical to a horizontal position, the effective stress at the measurement points reveals significant trends (Figure 7.5). Initially, both inner and outer bending stresses start low and increase gradually. In the middle region, minor fluctuations occur, but the stresses remain relatively close, indicating consistent stress distribution. Towards the end, both stresses spike sharply, with the inner bending stress reaching higher values due to compression. This suggests that the inner bend experiences greater stress concentrations during the transition.

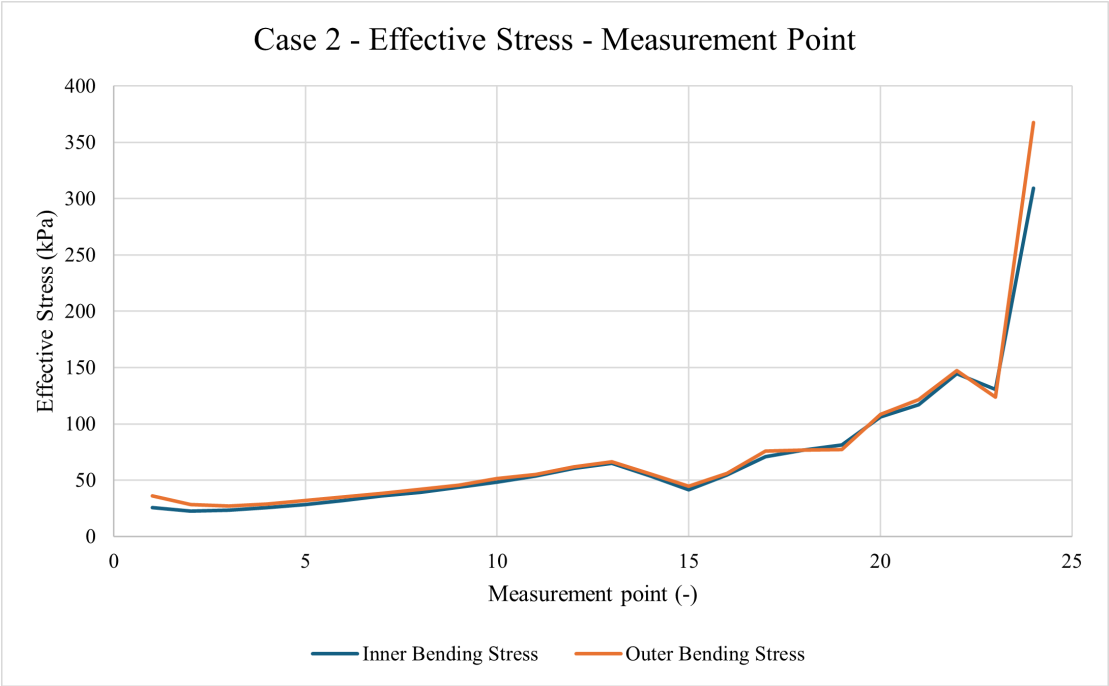

Figure 7.6: Result of Case 2 - Bending from Horizontal to Vertical (Upwards)

In case 2, which involves bending from a horizontal to a vertical position in an upward direction, a similar pattern is observed (Figure 7.6). The initial stress levels are low, with a slight increase at the beginning. In the middle region, the stresses remain close with minor fluctuations. Towards the end, a sharp increase in stress is noted, with the outer bending stress slightly higher than the inner bending stress. This indicates that the outer bend experiences more tension during the upward bending maneuver, highlighting the need for the probe to withstand tensile stresses effectively.

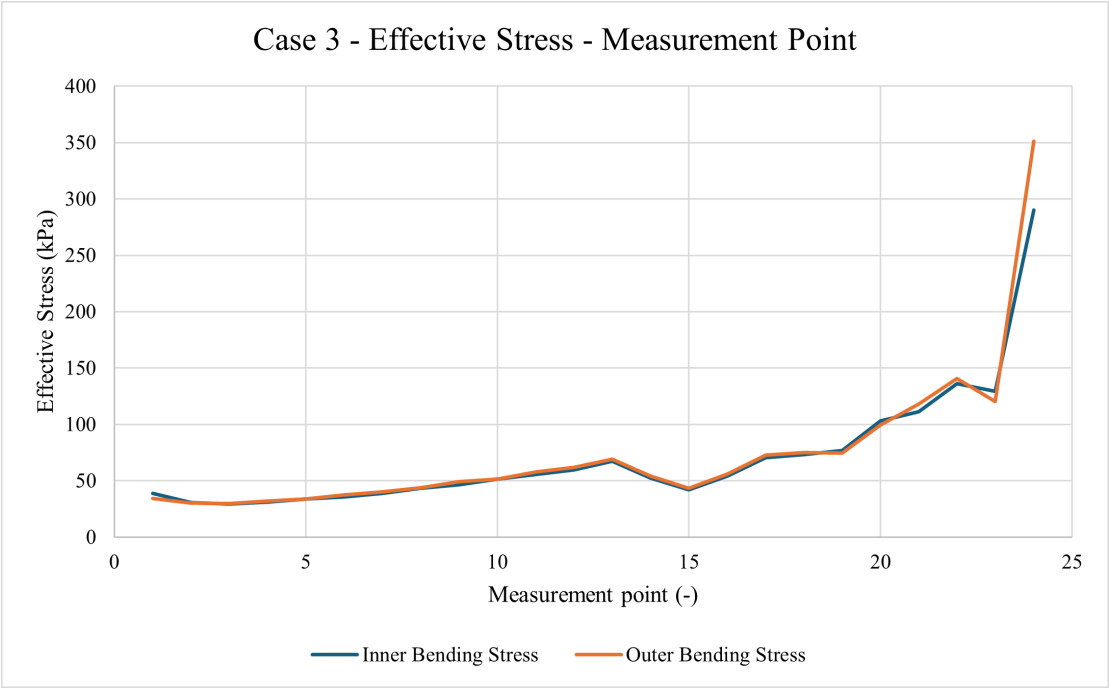

Figure 7.7: Result of Case 3 - Bending from Horizontal to Vertical (Upwards)

In case 3, where the probe bends from a horizontal to a vertical position in a downward direction, also shows comparable trends (Figure 7.7). The initial stress levels are low, with a slight increase. In the middle region, the stresses remain relatively close, with some fluctuations. Towards the end, a sharp increase in stress is observed, with the outer bending stress slightly higher than the inner bending stress. This indicates that the outer bend experiences more tension during the downward bending maneuver, similar to the upward bending scenario.

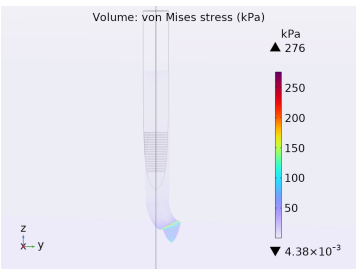

(a) Case 1 in COMSOL Simulation: Bending - Vertical to Horizontal

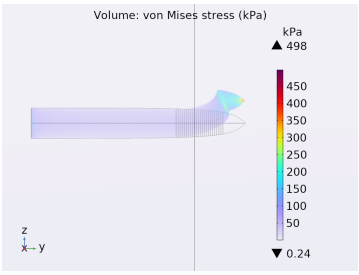

(b) Case 2 in COMSOL Simulation: Bending - Horizontal to Vertical - Upward

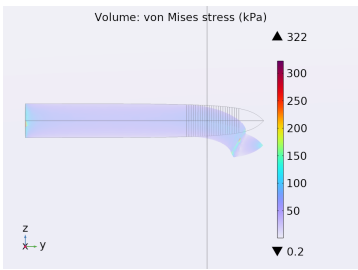

(c) Case 3 in COMSOL Simulation: Bending - Horizontal to Vertical - Downward

Figure 7.8: Different Cases of Bending in COMSOL Simulation

Furthermore, the COMSOL simulation 3D deformation result output can be seen in Figure 7.8. Figure 7.8a shows the result for Case 1 where bending occurs from vertical to horizontal. Figure 7.8b shows the result for Case 2 where bending occurs from horizontal to vertical upwards. Figure 7.8c shows the result for Case 3 where bending occurs from horizontal to vertical downwards. Moreover, a clearer overview of these cases in the COMSOL simulation can be seen in Appendix D.

7.4.1 Further Investigation

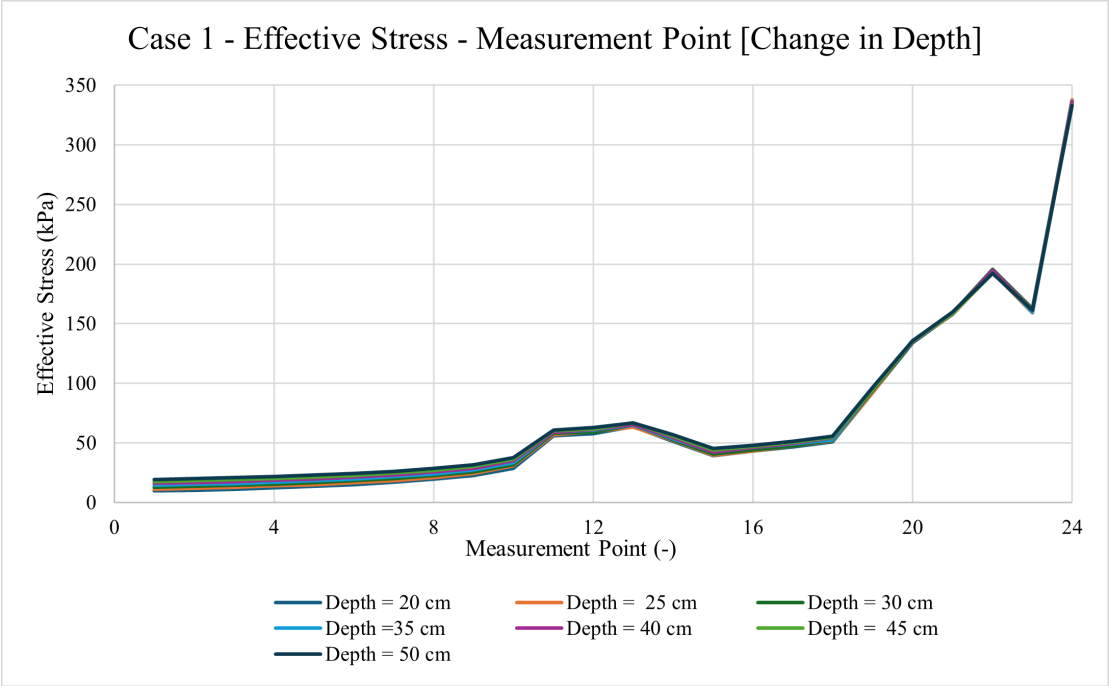

Figure 7.9: Case 1 - Effective Stress Distribution at Various Depths

The analysis of effective stress distribution at various depths, shown in Figure 7.9 reveals that changes in penetration depth do not significantly affect the stress values along the probe, which is unexpected. The expected result would be a more significant different with different depth.

Several potential reasons could explain why changes in depth do not significantly affect stress distribution. One possibility is the limitations of the COMSOL software or the mesh size used in the simulation. If the mesh is not fine enough, it may not capture subtle variations in stress distribution accurately. A more refined model setup with a finer mesh might provide more detailed insights into how depth affects stress distribution. Additionally, the current simulation only shows the inner stress. Including outer stress in the analysis could offer a more comprehensive understanding of the stress distribution along the probe.

7.5 Sensitivity Analysis

The sensitivity analysis aims to understand how variations in key parameters affect the effective stress experienced by the probe. The parameters considered include density, Young's modulus, and bending displacement. Each parameter is examined by changing its values, and the corresponding effective stress is analyzed and represented as a percentage change, as illustrated in Figure 7.10.

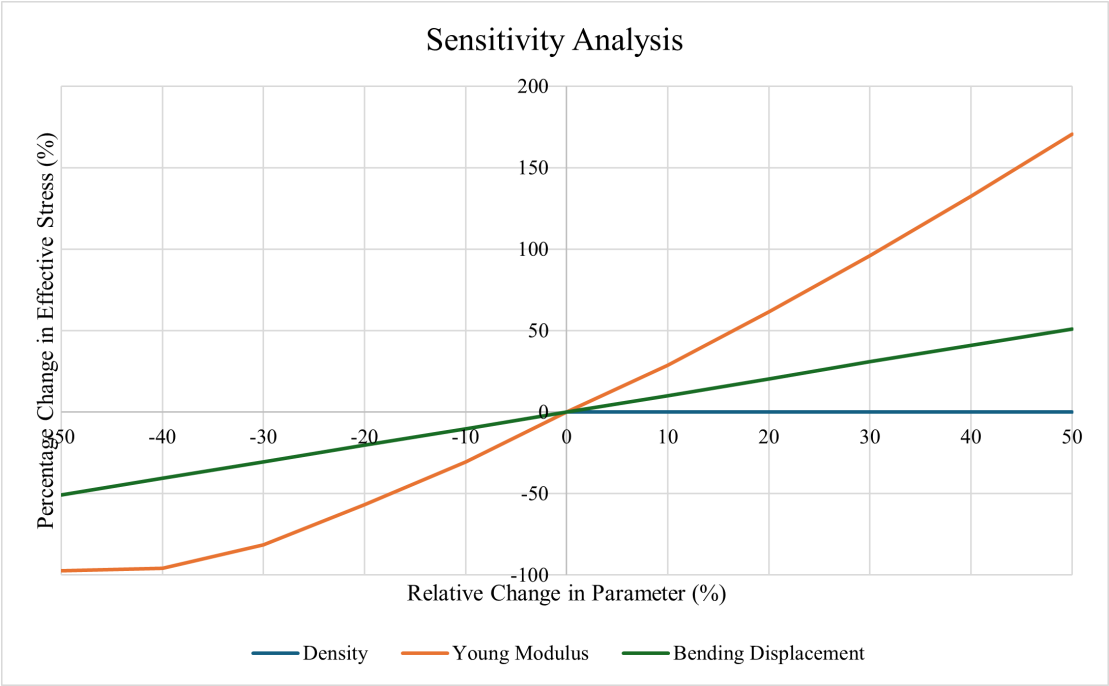

Figure 7.10: Sensitivity Analysis Performed on Density, Young Modulus, and Bending Displacement

At the initial simulation, or at 0 percent change, the density used is 1420 kg/m^3, which is the value calculated from the experimental setup. According to Cat.com (n.d.), the density of soil, such as wet gravel, can reach up to 2260 kg/m^3. Therefore, the sensitivity analysis is performed between 1420 kg/m^3 and 2260 kg/m^3, represented as a percentage increase in Figure 7.10, where 1420 kg/m^3 is represented as 0 percent. Unexpectedly, the change in soil density shows no significant impact on the effective stress, remaining almost constant across the range of changes. Usually, an increase in density should correlate with higher effective stress due to the increased mass and interaction forces within the soil. However, the unexpected constant trend might be attributed to limitations within the COMSOL simulation setup. Specifically, the inbuilt calculation algorithms in COMSOL may not accurately capture the influence of density variations on effective stress, Which leads to an underestimation of its impact.

For the Young's modulus of the soil, the value is adjusted by ± 50 percent because this range effectively captures the variability in soil stiffness and maintains appropriate physical meaning. However, since the value used in the simulation is significantly underestimated, as shown in Table C.1, it is calibrated so that the effective stress output aligns with the experimental value as explained in Section 7.1. Therefore, the change in value for the sensitivity analysis is based on the parameter value used in the simulation. The sensitivity analysis for changes in Young's modulus indicates a significant impact on effective stress. As Young's modulus increases, indicating a stiffer soil domain, the effective stress also increases. The stiffer the soil is, the higher the resistance to deformation, leading to a higher stress concentration, which is consistent with theoretical expectations. A stiffer soil resists deformation more, leading to higher stress concentrations, which is consistent with theoretical expectations.

The change in bending displacement on effective stress shows a moderate linear increase, reflecting the relationship between greater bending and increased stress. In the sensitivity analysis, the

initial bending displacement is set at 2.5 cm (0 percent), with -50 percent corresponding to 1.25 cm and +50 percent to 3.75 cm. As bending displacement increases, the effective stress rises due to more complex stress states within the probe and surrounding soil. This is because a greater bending introduces a higher localized stresses, particularly at points of maximum curvature, increasing the interaction between the probe and soil particles. This insight is important for designing soft robotic probes, because it emphasizes the need to account for bending dynamics in the probe's structural analysis. By utilizing how bending displacement affects stress, researchers can select appropriate materials and make geometric modifications to lower stress concentrations. This helps with the probe's durability and functionality in various soil conditions.

7.5.1 Anomalies

The anomaly observed with the density parameter highlights potential limitations within the COMSOL simulation environment. It is crucial to know that the built-in calculation methods in COMSOL might not fully account for the density variations, which leads to an under representation of their effect on effective stress. This limitation shows the need for careful consideration of simulation tools and methods when interpreting results.

8. Discussion

The analysis of the steering capacities of the rigid probe in dry sand provided crucial insights into its behavior under different operational conditions. The investigation focused on two main scenarios: penetration angle and bending maneuverability. Furthermore, The simulation is validated against experimental results, which confirms the accuracy of the COMSOL setup by comparing the effective stress experienced at the rigid tip. Moreover, to better simulate the interaction between the probe tip, the dry sand domain, and the surrounding environment, the boundary conditions are defined. The soil domain boundary investigation determined an optimal size of 30 cm in radius, which minimizes boundary influence.

In the penetration angle scenario, the analysis showed that changes in penetration direction significantly increase the effective stress experience on the probe from 384 to 1099 kPa varying from 0 degrees normal to the soil domain to 80 degrees. This highlights the importance of the fact that with different penetration angle, the resistance force on the probe is higher which can hinder the durability and the life-span of the probe. Selecting materials that balance flexibility and structural integrity, and investigating geometric designs, such as changing the aspect ratio of the tip in the tip chamber, can help distribute stress more evenly and improve the probe's steering capacity.

In the bending maneuverability scenario, it is observed that both inner and outer bending stresses increase towards the end of the maneuver. The outer bending stress tends to be slightly higher due to tension, which emphasizes the need for the tip to withstand tensile stresses effectively. For example, in Case 1 (vertical to horizontal), the peak stress observed in the inner bend of the probe is 336 kPa. In Case 2 (horizontal to vertical downwards), the peak stress observed in the outer bend is 368 kPa. In Case 3 (horizontal to vertical upwards), the peak stress observed in the outer bend is 351 kPa. This insight is important for designing tips capable of navigating complex soil environments while maintaining structural integrity. Smaller steering angles might result in lower stress concentrations, which improves the probe's durability and maneuverability. However, incorporating a model that accounts for deformation and rotation of the disks in the steering probe can provide more detailed insights into material design for the tip chamber of the earthworm soft robotic probe.

In summary, to answer the research question "How does dry sand soil influence the steering capabilities of a rigid probe tip for efficient soil penetration, as assessed through finite element modeling (FEM) using COMSOL software?", the investigation found that in the first scenario, the effective stress experienced by the rigid probe increases significantly as the penetration angle changes. Furthermore, in the second scenario of steering, it is observed that in all cases, there is peak stress experienced at the bend of the probe when steering. Both of these findings lead to the conclusion that the probe's steering capacity is highly dependent on the specific area or point that experiences peak stress. To improve the lifespan and steering capacity, the design of the soft robotic probe needs to select materials that can appropriately minimize the effect of the peak stress.

9. Conclusion

The thesis investigated the steering capacities of a rigid tip designed for a soft robotic probe in dry sand, focusing on the behavior of the probe under varying penetration angles and bending maneuvers. Through comprehensive FEM simulations using COMSOL Multiphysics, the investigation provided crucial insights into the effective stress distributions and the factors influencing them.

Firstly, the FEM simulation was validated against the experimental setup by comparing the effective stress at the rigid tip in both the simulation and the experiment. The parameter values were configured to ensure comparable outcomes. Additionally, an investigation of the soil domain boundary was conducted to determine an optimal size that minimizes boundary influence.

Secondly, the analysis of penetration angles showed that as the angle of penetration increases, so does the effective stress experienced by the probe tip. This finding underscores the importance of optimizing penetration angles to minimize stress, therefore enhancing the durability and operational efficiency of the probe.

Thirdly, the study of bending maneuverability showed that both inner and outer bending stresses increase significantly towards the end of the bending maneuver. The outer bending stress was found to be slightly higher due to the tension experienced during the maneuver. This indicates that the design of the probe tip must account for both compressive and tensile stresses to maintain its effectiveness. Ensuring the probe can withstand these stresses is important for its functionality in complex soil environments.

The sensitivity analysis highlighted that variations in Young's modulus and bending displacement significantly affect effective stress, whereas changes in soil density did not have a noticeable impact. This unexpected result suggests potential limitations within the COMSOL simulation environment, particularly regarding its inbuilt calculation methods. This limitation emphasizes the need for more consideration and possible validation of simulation results using different methods to ensure the reliability.

Future Work

Future work can build on these findings in many ways. Firstly, incorporating a more detailed model that accounts for the deformation and rotation of the small disks on the probe during steering could provide deeper insights into material design for the tip chamber of the earthworm-inspired soft robotic probe. Furthermore, simulating the behavior of the soil model from only elasticity to an elastic-plastic model could further encapsulate the realistic stress behavior experienced by the probe.

Further experimental validation with a broader range of soil types and conditions would be beneficial to assess the robustness and versatility of the probe design. Investigating different geometric configurations, such as altering the aspect ratio of the tip or the tip shape, can help distribute stress more evenly, improving maneuverability and durability, as well as determining which aspect ratio or tip shape is suitable for different soil conditions.

In conclusion, while this investigation provides valuable insights, it is not definitive that the current probe tip shape and model are the best for the concept of an earthworm-inspired soft robotic probe, as not all possible scenarios have been explored. However, this research lays the groundwork for further studies aimed at determining the optimal probe tip shape for various

conditions. To enhance the feasibility and optimization of the earthworm-inspired soft robotic probe, it is recommended to continue with extensive research and development. This approach will ultimately make the probe a highly valuable tool in geotechnical engineering and related fields.

Bibliography

American Society for Testing and Materials (ASTM). (2007). *Standard Test Method for Particle-Size Distribution (Sieve Analysis) of Soils (D422-63)*.

Anselmucci, F., Venus, S., Sadeghi, A., & Magnanimo, V. (2022). A Robotic Earthworm to Explore the Underground: Design, Fabrication and Testing [Alert Geomaterial].

Cat.com. (n.d.). Earthwork Volumes Reference Tables [Accessed: 2024-06-24].

Coulomb, C. (1776). Essai sur une application des regles des maximis et minimis a queles problemes de statique relatifs a l'architecture. *Mémoires de l'Académie Royale des Sciences*.

Erkens, G., & Stouthamer, E. (2020). The 6m approach to land subsidence. *Proceedings of the International Association of Hydrological Sciences*, *382*, 733–740. https://doi.org/10.5194/piahs-382-733-2020

eSUN. (2024). *PLA+ Filament Technical Data Sheet* [Version 4.0]. https://www.esun3d.net/filament/esun-pla+

Fong, J. (2019). The advantages of the finite element method [IEEE Innovation at Work]. https://innovationatwork.ieee.org/the-advantages-of-fem/

Geoprobe. (n.d.). CPT Cone Penetration Testing [Accessed: 2024-06-15].

Han, J., & Ma, Q. (2019). Finite Element Analysis of geotechnical excavation based on Comsol Multiphysics. *IOP Conference Series: Materials Science and Engineering*, *592(1)*, 012060. https://doi.org/10.1088/1757-899x/592/1/012060

Isaka, K., Tsumura, K., Watanabe, T., Toyama, W., Sugesawa, M., Yamada, Y., Yoshida, H., & Nakamura, T. (2019). Development of underwater drilling robot based on Earthworm locomotion. *IEEE Access*, *7*, 103127–103141. https://doi.org/10.1109/access.2019.2930994

Labuz, J. F., & Zang, A. (2012). Mohr–coulomb failure criterion. *Rock Mechanics and Rock Engineering*, *45(6)*, 975–979. https://doi.org/10.1007/s00603-012-0281-7

Liu, H., Chu, J., & Kavazanjian, E. (2023). Biogeotechnics: A new frontier in geotechnical engineering for Sustainability. *Biogeotechnics*, *1(1)*, 100001. https://doi.org/10.1016/j.bgtech.2023.100001

Lunne, T., Powell, J. J. M., & Robertson, P. K. (1997). *Cone Penetration Testing in Geotechnical Practice*. Chapman; Hall/CRC.

Patino-Ramirez, F., & O'Sullivan, C. (2022). Optimal tip shape for minimum drag and lift during horizontal penetration in granular media. *SSRN Electronic Journal*. https://doi.org/10.2139/ssrn.4247930

Tekin, A. (2024). Experimental Measurement of Soil-Intruder Interactions for Soft Robots Design [University of Twente Internal research].

Zhang, W., Huang, R., Xiang, J., & Zhang, N. (2024). Recent advances in bio-inspired geotechnics: From burrowing strategy to underground structures. *Gondwana Research*, *130*, 1–17. https://doi.org/10.1016/j.gr.2023.12.018

Zienkiewicz, O. C., Taylor, R. L., & Zhu, J. (2005). *The Finite Element Method for Solid and Structural Mechanics*. Elsevier.

Appendix A: Primary Soil Data

A.1 Weight of Soil in Each Sieve

Table A.1 presents the weight of soil retained in each sieve for three different trials. The sieves have varying diameters of openings, ranging from 4 mm to 0.063 mm. The data shows the distribution of soil particle sizes, which is essential for understanding the soil's granular composition.

- **Diameters of Opening (mm)**: The size of the sieve openings through which soil particles pass.
- **Try 1 (g)**, **Try 2 (g)**, **Try 3 (g)**: The weights of soil retained in each sieve for three separate trials.

The total weight of the soil for each trial is also provided, ensuring the consistency and reliability of the sieving process.

Table A.1: Weight of Soil in Each Sieve

Diameters of Opening (mm)	Try 1 (g)	Try 2 (g)	Try 3 (g)
4	8.02	14.61	9.63
2	10.04	23.55	18.79
1.4	17.25	29.04	29.97
1	41.53	82.61	57.05
0.85	1771.44	1092.8	1501.99
0.5	1728.85	1930.1	2299.82
0.3	935.9	1175.11	640.78
0.25	27.91	44.65	13.49
0.125	176.31	186.41	88.31
0.09	8.66	19.7	4.21
0.063	3.19	0.95	1.49
0	6.8	3.59	2.68
Total weight	**4735.9**	**4603.12**	**4668.21**

A.2 Calculations for Shearing Test

Table A.2 includes the calculations necessary for conducting the shearing test on the soil samples. The parameters measured include the weight of the sand, the specific volume (Vs and Vv), void ratio (e), normal stress applied, and the resulting maximum shear stress in Newtons and kilopascals (kPa).

- **Weight sand (g)**: The weight of the sand used in the shearing test.
- **Vs and Vv**: Specific volumes of solids and voids.
- **e**: Void ratio, indicating the proportion of voids in the soil sample.

- **Normal stress applied (kPa)**: The pressure applied to the soil during the shearing test.
- **Maximum shear stress (N, kPa)**: The highest shear stress recorded during the test, in both Newtons and kilopascals.

Sample Calculation of Weight Applied to Normal Stress Conversion in kPa

The formula used to calculate the normal stress (σ) applied is as follows:

$$\sigma = \left(\frac{W}{g} + H\right) \times \frac{1}{A} \times C$$

where:

- σ = Normal Stress (kPa)
- W = Applied Weight (N)
- g = Acceleration due to gravity (9.805 m/s^2)
- H = Hanger Weight (kg)
- A = Surface Area of the Box (mm^2)
- C = Conversion Factor from kg/mm^2 to kPa (9.805×10^3)

Using the given values: $W = 80$ N, $H = 5.03$ kg, $A = 3136$ mm^2:

$$\sigma = \left(\frac{80}{9.805} + 5.03\right) \times \frac{1}{3136} \times 9.805 \times 10^3 = 41.237\,\text{kPa}$$

This equation calculates the normal stress applied in kPa based on the applied weight, hanger weight, and surface area of the box.

Summary of Direct Shearing Test Values

Table A.2: Calculations for Shearing Test

Weight sand	**Vs**	**Vv**	**e**	**Normal stress Applied (kPa)**	**Maximum shear stress (kPa)**
155.990	58.864	47.760	0.811	22.104	21.593
157.910	59.589	47.035	0.789	28.482	29.020
155.490	58.675	47.949	0.817	41.237	35.714

Appendix B: Material Properties of the Probe (PLA)

Material Properties of the Probe (PLA)

Table B.1 outlines the material properties of the PLA (Polylactic Acid) used to construct the rigid tip of the soft robotic probe.

The key properties listed are:

Density (kg/m^8): The mass per unit volume of the PLA material.

Young's modulus (MPa): The measure of the stiffness of the PLA material, indicating its ability to deform elastically when a force is applied.

These material properties are vital for accurately modeling the probe's behavior in the numerical simulations and ensuring its performance during soil penetration tests.

Table B.1: Material Properties of the Probe (PLA)

Property	**Value**	**Unit**
Density	1230	kg/m^3
Young's modulus	1973	MPa

More data regarding the material of the rigid tip used in the experiment and the simulation can be found in the manual of eSuneSUN, 2024.

Appendix C: COMSOL Geometry Setup and Parameter Configuration

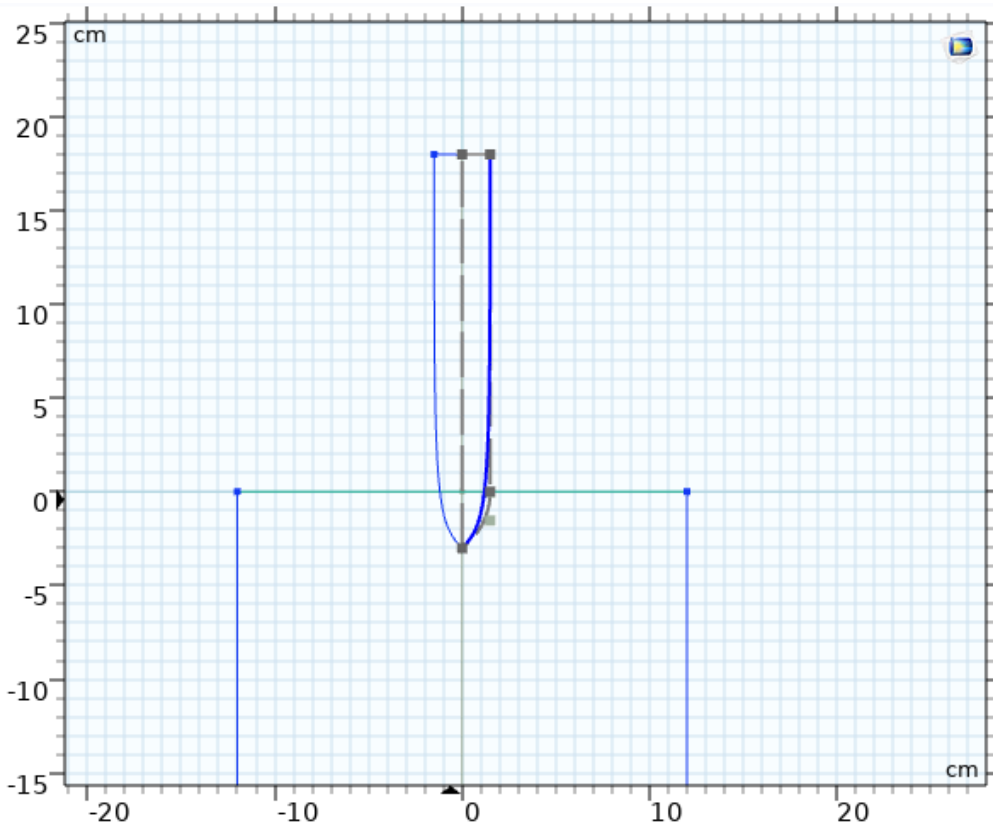

Figure C.1: Geometry Setup in COMSOL - 1

The geometric setup in COMSOL for the probe simulation is illustrated in Figure C.1. The grey lines represent construction lines used for reference, while the blue line indicates the actual geometry of the probe and soil domain. The use of a smooth line for the geometry helps to avoid anomalies in COMSOL simulations, which is important for accurately modelling the interaction between the probe and the soil.

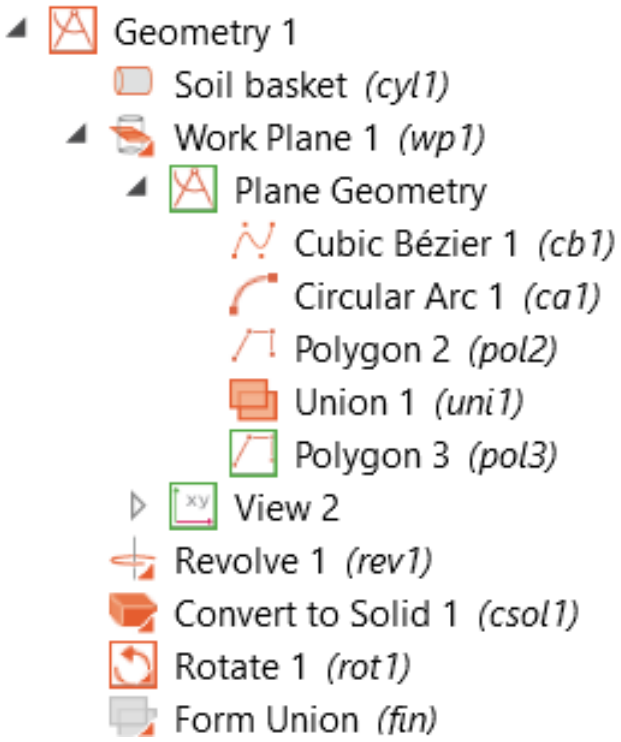

Figure C.2: Geometry Set Up in COMSOL - 2

Figure C.2 displays the geometry tree in COMSOL, showing the various components used to construct the model. Key elements include the soil basket (cyl1), work plane (wp1), and various geometric shapes such as the cubic Bézier curve (cb1), circular arc (ca1), and polygons (pol2, pol3). The process involves creating these shapes, uniting them (uni1), converting to solid (csol1), rotating (rot1), and finally forming a union (fin) to complete the model.

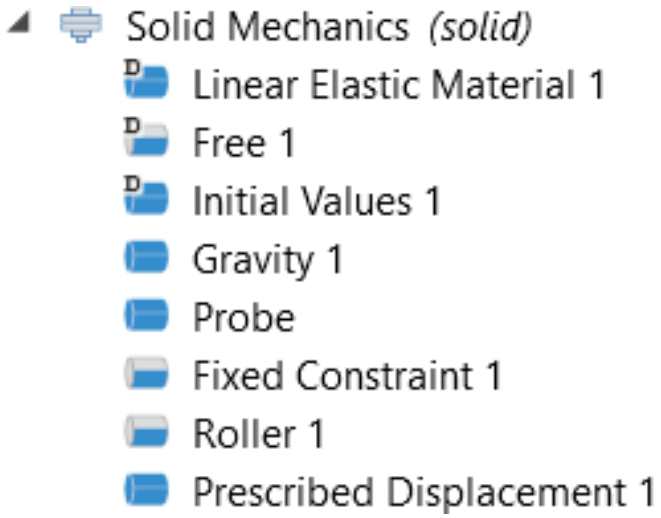

Figure C.3: Physics Setup

he physics setup for the COMSOL simulation is depicted in Figure C.3. It includes the definition of solid mechanics (solid) with key elements such as linear elastic material properties (Linear Elastic Material 1), initial values (Initial Values 1), gravity effects (Gravity 1), and boundary conditions like fixed constraints (Fixed Constraint 1) and rollers (Roller 1). The prescribed displacement (Prescribed Displacement 1) defines the movement applied to the probe.

Table C.1 lists the parameters used in the probe simulation. The value for Young's Modulus is significantly underestimated to ensure the output of the results is comparable with the experimental data. The rest of the data are consistent with the experimental setup described in the report.

Table C.1: Parameters for Probe Simulation

Name	**Value**	**Unit**	**Description**
dsp	0.2	m	Displacement of the probe
E_y0	35000	Pa	Young Modulus
theta	0	deg	Penetration angle
rho0	1420	kg/m^3	Bulk Density

Appendix D: COMSOL Deformation Simulation Result Output for Steering Capacity Scenario 2: Steering

This appendix presents the results of the COMSOL deformation simulations conducted to evaluate the steering capacity of the rigid probe under various bending scenarios. The purpose of these simulations is to analyze the von Mises stress distribution within the soil domain when the probe undergoes different bending maneuvers. The three bending cases investigated are:

1. Bending from a vertical to a horizontal position.
2. Bending from a horizontal to a vertical position in an upward direction.
3. Bending from a horizontal to a vertical position in a downward direction.

Figures D.1, D.2, and D.3 below illustrate the von Mises stress distribution for each bending scenario, providing insights into the areas of high stress concentration and the overall behavior of the probe within the soil.

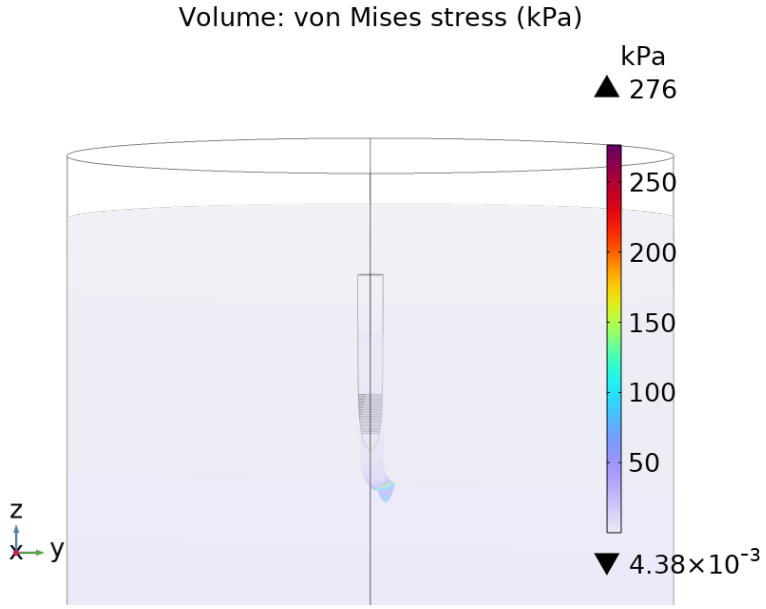

Figure D.1: Case 1 in COMSOL Simulation: Bending - Vertical to Horizontal

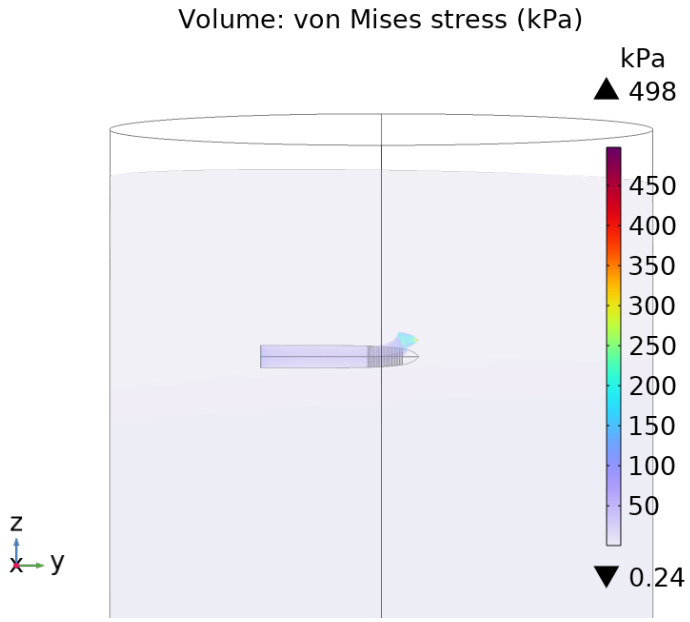

Figure D.2: Case 2 in COMSOL Simulation: Bending - Horizontal to Vertical - Upward

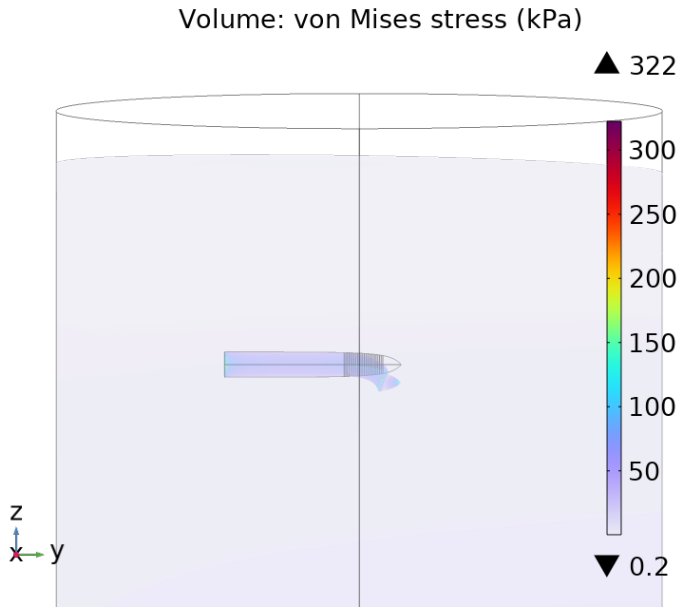

Figure D.3: Case 3 in COMSOL Simulation: Bending - Horizontal to Vertical - Downward